



Deceleration of SO₂ poisoning on PtPd/Al₂O₃ catalyst during complete methane oxidation

Nadezda Sadokhina^a, Gudmund Smedler^b, Ulf Nylén^c, Marcus Olofsson^d, Louise Olsson^{a,*}

^a Chemical Engineering, Chalmers University of Technology, SE-412 96 Gothenburg, Sweden

^b Johnson Matthey AB, SE-421 31 Västra Frölunda, Sweden

^c Scania CV AB, SE-151 87 Södertälje, Sweden

^d AVL MTC Motortestcenter AB, Box 223, SE-136 23 Haninge, Sweden



ARTICLE INFO

Keywords:

Methane oxidation
Noble metal
Inhibition
Promotion
Sulfur poisoning

ABSTRACT

The inhibiting effect of SO₂ on the catalytic activity of the monometallic Pt/Al₂O₃ and Pd/Al₂O₃, as well as on bimetallic PtPd/Al₂O₃ catalyst for the complete oxidation of methane under lean conditions has been studied. Flow reactor experiments, *in-situ* DRIFT spectroscopy and characterization with XPS, STEM-EDX were performed. It was found that the addition of Pt to the Pd/Al₂O₃ resulted in a catalyst that was more robust towards sulfur poisoning. XPS results revealed residual sulfates on catalyst surface after regeneration. This was confirmed with EDX analysis, which demonstrated that sulfur was accumulated in noble metal particles and especially in the region of the particle rich in Pt. Although the catalyst has been deactivated in the presence of both SO₂ and H₂O, an additional presence of NO in the gas mixture of reactants resulted in an increased lifetime of the sample under reaction conditions. This NO effect strongly depends on the temperature of experiments and is most intense at a temperature close to 550 °C A postponed inhibition caused by the addition of NO may be explained by the DRIFTS results, which demonstrated that the presence of NO lowers the sulfate formation and mostly surface sulfites are observed that increase the lifetime of the catalyst during SO₂ exposure.

1. Introduction

Sulfur-containing components of fuels are well-known poisons for catalytic materials utilized in emission control [1–8]. The retrieval of catalytic activity and the preservation of catalytic performance are the subject of current intensive research particularly in the connection with aftertreatment of natural gas-powered vehicle (NGV) exhaust [9–14]. Due to the potential for much lower emissions of CO₂, particulate matter and especially NO_x, lean-burn natural gas engines have been developed to compete with diesel engines [7]. The function of a catalytic converter in this case is to oxidize unburned CH₄ and remove it from the exhaust. However, the efficiency of the converter is affected by even small amounts of SO₂ released as a result of the fuel combustion under excess of oxygen [4,15]. If poisoning has occurred, the catalyst is required to be regenerated and the optimal regeneration procedure should be addressed as well.

It is well-known that supported palladium catalysts demonstrate high activity during complete methane oxidation. Based on a literature review, it becomes evident that under O₂ excess, palladium oxide plays an active part, whereas metallic palladium is much less active under the same conditions [4,5,16–20]. However, methane oxidation activity of

Pd-based materials decreases over time in the presence of water and sulfur-containing compounds in the exhaust gas [15,21–25]. In the case of water inhibition, adsorption of water and continuous formation of hydroxyls on PdO surface, as well as on Al₂O₃, provide an explanation of the catalytic activity loss. In the case of SO₂-poisoning, it is agreed that PdO-based catalysts are deactivated through the oxidation of SO₂ to SO₃ on PdO followed by the formation of sulfates on Pd blocking active sites, which further migrate to Al₂O₃ forming Al₂(SO₄)₃ [4,9,21]. Moreover, in the presence of both H₂O and SO₂, the joint inhibiting effect is also reported in the literature [21,26], indicating that activity loss was greater and occurred more rapidly when both poisons are included into the gas feed.

In addition, Pt was chosen to increase the resistance of the Pd-based catalyst to inhibition by H₂O [27–32] and to SO₂ poisoning [11,33,34]. Greater resistance of bimetallic materials to sulfur poisoning may be related to the ability of metallic Pt to adsorb SO₂. Therefore, the presence of metallic Pt may prevent the adsorption of sulfur dioxide on Pd surface sites which are then available for methane oxidation [12]. However, there is an optimal content of Pt that can be added to Pd-based material [11,31,35–37]. Recently the regeneration of S-poisoned PtPd-based catalyst was studied by Wilburn and Epling [11] which

* Corresponding author.

E-mail address: louise.olsson@chalmers.se (L. Olsson).

showed that effectiveness of SO₂ regeneration methods decreased with increasing Pt content.

It was previously demonstrated that the presence of NO significantly slows down the rate of deactivation of catalysts by water vapor. Our previous study [38] showed that the deactivation of Pd/Al₂O₃-based catalysts by water under excess of O₂ could be retarded by adding nitric oxide to the gaseous mixture of the reactants. Nitric oxide may react with surface hydroxyls to form reactive surface species that facilitate methane oxidation. It may also be adsorbed on PdO, which slows the formation of –OH on the support. However, to our knowledge there are no studies available that have examined the effect of NO on the catalyst deactivation by SO₂ itself or by the joint presence of H₂O and SO₂.

The objective of the current study is to focus on the NO and SO₂ interaction over a Pd-based catalyst under conditions of methane oxidation in the presence of O₂ excess. The high-loaded monometallic Pd/Al₂O₃, Pt/Al₂O₃ and bimetallic PtPd/Al₂O₃ catalysts in monolith form were studied by flow reactor experiments, as well as by *in-situ* DRIFT spectroscopy. In addition, catalyst characterization with XPS and STEM-EDX was performed.

2. Experimental part

2.1. Catalyst preparation and characterization

Powder samples were prepared using wet impregnation (“WI”) of commercial γ-Al₂O₃ (Sasol, Puralox SBa-200) calcined at 900 °C for 2 h in the oven. Initially, a slurry of support material was prepared, with pH stabilized at 4 using a diluted HNO₃ solution. In addition, Pt- and Pd-precursor solutions were prepared by a dilution of Pt(NO₃)₂ (Heraeus GmbH, 15.12 wt.% Pt) and Pd(NO₃)₂ (Heraeus GmbH, 17.27 wt.% Pd) in MilliQ water. The precursor solution was added dropwise to the support slurry and was stirred for 1 h at a pH of 2. After stirring, the solution was frozen with liquid nitrogen and dried under vacuum. The powder obtained was calcined at 500 °C for 2 h in the oven. The powder of the bimetallic catalysts was prepared by a sequential wet impregnation method to obtain first 1.9 wt.% Pt and then 3.8 wt.% Pd, whereas the noble metal loading in monometallic samples corresponding to the same amount of metal in the bimetallic sample (i.e. 1.9 wt.% Pt/Al₂O₃ and 3.8 wt.% Pd/Al₂O₃). For simplicity, the samples will hereafter be referred to a batch “WI”.

For comparison, another batch of 3.8 wt.% Pd/Al₂O₃ and 1.9 wt.% Pt-3.8 wt.% Pd/Al₂O₃ catalyst was synthesized by incipient wetness impregnation (“IWI”) method using the same noble metal precursors and Al₂O₃ support followed by drying at 80 °C overnight and thereafter calcination at 500 °C for 2 h in the oven. Bimetallic samples were prepared by a two-step IWI starting with Pd first and then with Pt, with drying and calcination between the addition of each metal. These samples were used only for a few experiments (shown in Figs. 5 and S3) to demonstrate inhibition/poisoning /promotion effects were present for catalysts prepared with different methods. These catalysts will be referred in a text to batch “IWI”.

The powder obtained was placed on ceramic monoliths (D = 21 mm, L = 20 mm; 400 cpsi) using the following procedure. A slurry of 20 wt.% dry content (catalyst powder and ‘binder’ (Sasol, Disperal P2) at a 4:1 ratio) was prepared by mixing the solid phase with a solution of ethanol and distilled water (the ratio of pure ethanol to water was 1:1). The monoliths were calcined at 600 °C for 2 h prior to the washcoating. The monoliths were coated with catalyst slurry by immersing the monolith into the slurry, blowing away excess slurry by air flow, drying it at 100 °C for 2 min and calcining it at 600 °C for 2 min using a hot gun. This procedure was repeated until the monoliths had been coated with the desired amount of washcoat (mass of washcoat = 500 ± 10 mg). The monoliths covered by washcoat were then calcined at 600 °C for 2 h in the oven.

A transmission electron microscopy (TEM) analysis was performed to examine the particle size of the PtPd/Al₂O₃ catalysts, as well as

examining whether any alloys had been formed between Pt and Pd particles. For the TEM analysis, the powder of the sample was collected from the SO₂-poisoned monolith after it had been regenerated under reducing conditions (see description below in the Section 2.2). The sample was pestled in an agate mortar and then placed on carbon films using TEM Cu grids. The particles were imaged using an FEI Titan 80-300 TEM with a probe Cs (spherical aberration) corrector operated at 300 kV. The images were recorded using a high angle annular dark field (HAADF) detector in the scanning TEM imaging mode (STEM), providing a Z number contrast. The electron probe size was about 0.2 nm for this study. The elemental analysis of the particles was performed by energy dispersive X-ray (EDX) spectroscopy. Open software ImageJ was used for processing STEM images and accounting particle size distribution. Dispersion of noble metals was calculated based on average particle size using formula described elsewhere [39,40].

XPS measurements were performed to examine oxidation state of the noble metals and chemical composition of the samples using a Perkin Elmer PHI 5000C ESCA system equipped with monochromatic Al Kα X-ray source with a binding energy of 1486.6 eV. For reference, the C 1 s with a binding energy of 284.6 eV was used. Peaks deconvolution was performed using CasaXPS software. The powder for the analysis was collected from the same monolith as for the STEM analysis.

2.2. Catalytic activity measurements

Experiments were performed in a fixed-bed flow reactor. The monolith samples (D = 21 mm; L = 20 mm) were placed in a quartz tube with an inner diameter of 22 mm and a length of 800 mm, equipped with an insulated heating wire controlled by a Eurotherm temperature controller. The temperature was measured by two thermocouples; the first positioned in the center of the sample and the second placed 10 mm upstream of the monolith. The temperatures presented in this paper have been derived from the thermocouple that had been placed in the middle of the monolith. The total gas flow was held constant at 3.5 l/min which corresponds to 210 l/h and gives approximately 30,000 h⁻¹ as a gas hour space velocity (GHSV), controlled by a system of Bronkhorst mass flow controllers. Water was evaporated and dosed by the CEM (controlled evaporator and mixer) system (Bronkhorst High-Tech B.V.). The outlet gas composition was monitored using an MKS MultiGas 2030 HS FTIR gas analyzer.

2.2.1. Degreening (refers to A in Fig. 1)

Before first tests to stabilize catalytic activity and prevent its changes under experimental conditions, fresh synthesized samples were degreened under the same conditions using the following procedure:

- (1) heating in the flow of Ar followed by reduction at 500 °C in 2 vol. % H₂ in Ar for 30 min;
- (2) treatment at 700 °C under lean conditions (500 ppm CH₄, 500 ppm NO, 8 vol.% O₂, 300 ppm CO, 5 vol.% H₂O, Ar) for 60 min;
- (3) treatment at 700 °C under rich conditions (2 vol.% H₂, 5 vol.% H₂O, Ar) for 20 min;
- (4) repeating the treatment in step (2) followed by treatment in Ar flow for 10 min.

2.2.2. Temperature-programmed activity tests (refers to B in Fig. 1)

The gas mixture used in the activity tests consisted of 500 ppm CH₄, 8 vol.% O₂, 5 vol.% H₂O, and Ar, and was named as the ‘initial gas mixture’. The procedure for activity tests was:

- (1) pre-treatment of the catalyst at 700 °C using 8 vol.% O₂ in Ar flow for 30 min followed by cooling to 150 °C in Ar flow;
- (2) activity test with a temperature ramp from 150 to 700 °C (heating step) and back to 150 °C (cooling step) at a rate of 5°/min using the initial gas mixture;
- (3) repeating the temperature ramp in step (2).

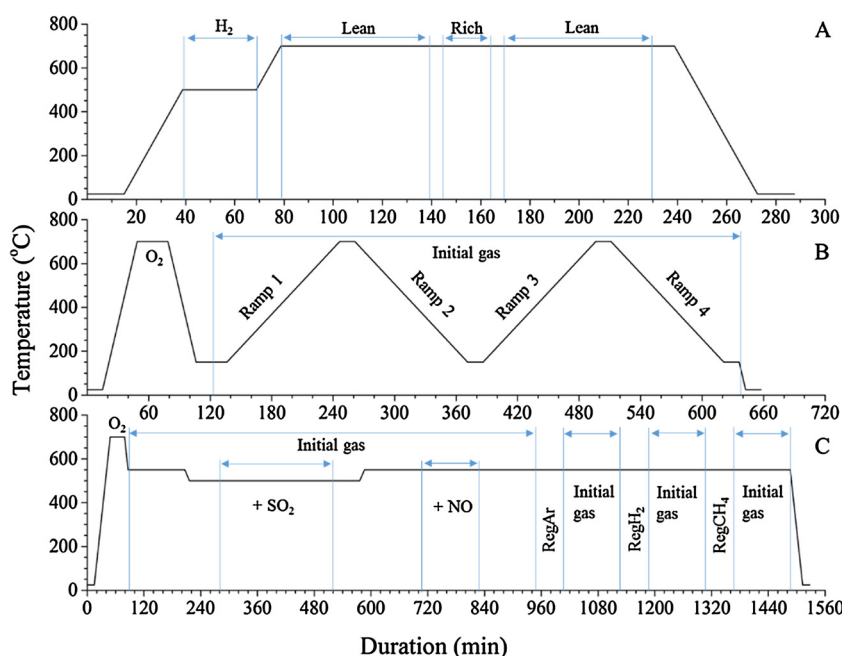


Fig. 1. Reaction protocol for (A) degreening; (B) temperature-programmed activity tests; (C) constant temperature and regenerated sample activity tests.

Heating and cooling performed during step (2) are referred in the Discussion section as ramp 1 and ramp 2, respectively. Heating and cooling performed during step (3) are referred in the Discussion section as ramp 3 and ramp 4, respectively.

2.2.3. Constant temperature activity tests (refers to C in Fig. 1)

The procedure for constant temperature activity tests of the samples was:

- (1) pre-treatment of the catalyst at 700 °C using 8 vol.% O₂ in Ar flow for 30 min followed by cooling to 550 °C in Ar flow;
- (2) activity test at 550 °C using the initial gas mixture (see above) for 2 h followed by a decrease of temperature to 500 °C in the same gas mixture;
- (3) activity test at 500 °C using the initial gas mixture for 1 h;
- (4) SO₂-poisoning performed at 500 °C using the initial gas mixture with an addition of 10 ppm SO₂ for 4 h;
- (5) repeating the activity test in step (3) followed by an increase in temperature to 550 °C in the same gas mixture;
- (6) repeating the activity test in step (2);
- (7) repeating the activity test in step (2) with the addition of 500 ppm NO to the initial gas mixture;
- (8) repeating the activity test in step (2).

2.2.4. Regenerated sample activity tests (refers to C in Fig. 1)

The procedure for the regeneration of the samples was performed directly after the above described activity and poisoning tests and consisted of the following steps:

- (9) treatment in Ar flow at 550 °C for 1 h;
- (10) repeating the activity test in step (2);
- (11) treatment in 2000 ppm H₂ in Ar flow at 550 °C for 1 h;
- (12) repeating the activity test in step (2);
- (13) treatment in 500 ppm CH₄ in Ar flow at 550 °C for 1 h;
- (14) repeating the activity test in step (2).

2.2.5. Detailed activity tests (with NO) type 1 (refers to Fig. 2)

The NO effect was studied in greater detail for the 1.9%Pt-3.8%Pd/ Al_2O_3 catalyst. For each SO₂ poisoning experiment, a new monolith containing powder from the same batch was used to avoid the influence

of the sulfates left on the surface. The procedure to investigate the NO effect on the catalytic activity of the S-poisoned PtPd/ Al_2O_3 only sample was:

- (1) pre-treatment of the catalyst at 700 °C using 8 vol.% O₂ in Ar flow for 30 min followed by cooling to 550 °C in 8 vol.% O₂ in Ar flow;
- (2) activity test at 550 °C using initial gas mixture for 1 h;
- (3) SO₂-poisoning performed at 550 °C using the initial gas mixture with an addition of 10 ppm SO₂ for 1 h;
- (4) regeneration in 500 ppm CH₄ in Ar flow at 550 °C for 1 h;
- (5) repeating the SO₂-poisoning in step (3);
- (6) repeating the regeneration in step (4);
- (7) repeating the SO₂-poisoning in step (3) with addition of 500 ppm NO;
- (8) repeating the regeneration in step (4);
- (9) repeating the SO₂-poisoning in step (7).

The NO effect was further examined using a new monolith in experiments in which 500 ppm NO was added to steps (2), (3), (5).

2.2.6. Detailed activity tests (with NO) type 2 (refers to Fig. 2)

Another type of experiment at 550 °C was performed:

- (1) pre-treatment of the catalyst at 700 °C using 8 vol.% O₂ in Ar flow for 30 min followed by cooling to 550 °C in 8 vol.% O₂ in Ar flow (the sample that was not exposed to NO was cooled in Ar flow only);
- (2) activity test at 550 °C using the initial gas mixture for 4 h;
- (3) SO₂-poisoning performed at 550 °C using the initial gas mixture with an addition of 10 ppm SO₂ for 4 h;
- (4) activity test at 550 °C using the initial gas mixture for 4 h;
- (5) regeneration in 500 ppm CH₄ in Ar flow at 550 °C for 1 h;
- (6) activity test at 550 °C using initial gas mixture for 1 h.

The NO effect was tested in additional experiments in which 500 ppm NO was added to steps (2), (3) using a new monolith.

2.2.7. Detailed activity tests (with NO) type 3 (refers to Fig. 2)

The mutual effect of H₂O, SO₂ and NO was studied at 450 °C. The

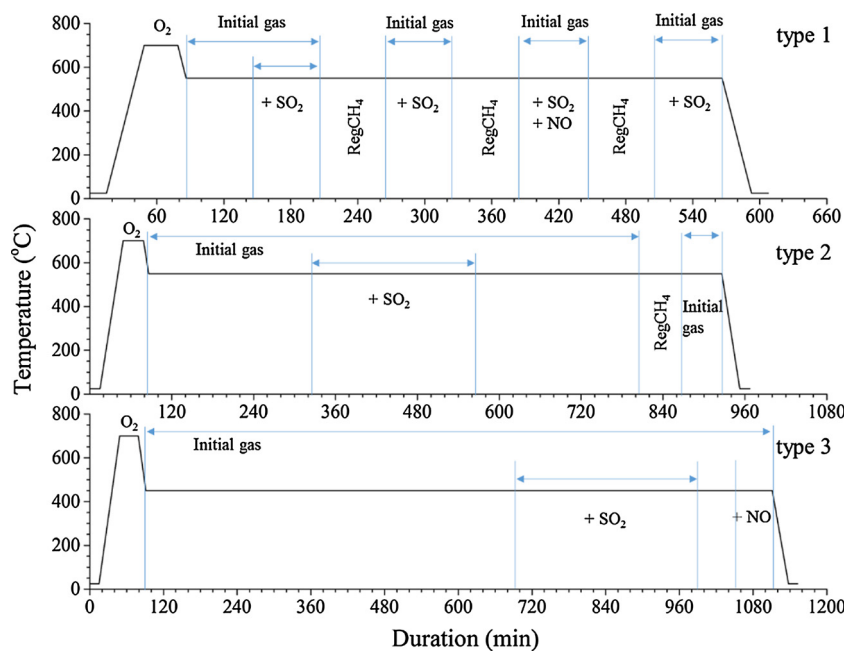


Fig. 2. Reaction protocol for detailed activity tests (with NO) types 1, 2 and 3.

experimental procedure consisted of the following steps:

- (1) pre-treatment of the catalyst at 700 °C using 8 vol.% O₂ in Ar flow for 30 min followed by cooling to 450 °C in 8 vol.% O₂, in Ar flow;
- (2) activity test at 450 °C using the initial gas mixture for 10 h;
- (3) SO₂-poisoning performed at 450 °C using the initial gas mixture with an addition of 10 ppm SO₂ for 5 h;
- (4) activity test at 450 °C using the initial gas mixture for 1 h;
- (5) activity test at 450 °C using the initial gas mixture with addition of 500 ppm NO for 1 h.

The NO effect was tested in experiments in which 500 ppm NO was added to steps (2) and (3) using a new monolith.

2.3. Spectroscopic measurements

Diffuse Infra-Red Fourier Transform Spectroscopy (DRIFTS) was conducted to investigate surface species formed on the catalyst during methane oxidation. The spectra were recorded on an FTIR spectrometer (Vertex 70, Bruker), coupled with a system of Bronkhorst mass flow controllers to deliver required gas composition.

Prior to the measurements, the sample powder was degreened using a ceramic crucible in the flow reactor in the same way as fresh synthesized monolith (see Section 2.2); to obtained SO₂-poisoned samples the degreening was followed by SO₂-poisoning at 450 °C with initial gas mixture consisted of 500 ppm CH₄, 8 vol.% O₂, 5 vol.% H₂O, 10 ppm SO₂ and Ar. Thereafter, the powder of the sample was mixed with KBr powder (1:1 mass ratio) followed by forming a solid pellet which then was crushed and sieved to give particle sizes between 40 and 80 µm. The tests were carried out using a total gas flow of 200 ml/min.

The procedure for the IR spectra recording consisted of the following steps:

- (1) pre-treatment of the catalyst at 550 °C using 2 vol.% O₂ in Ar flow for 1 h followed by cooling to 450 °C in Ar flow;
- (2) activity test at 450 °C for 40 min using 1000 ppm CH₄, 1.5 vol.% O₂, 1 vol.% H₂O in Ar flow followed by recording the ground spectrum;
- (3) heating in the same gas mixture up to 500 °C;

- (4) SO₂-poisoning using 1000 ppm CH₄, 1.5 vol.% O₂, 1 vol.% H₂O, 500 ppm SO₂ in Ar flow and 1000 ppm NO if added at 500 °C for 1.5 h accompanied by spectra recording every 15 s.

3. Results and discussion

3.1. Resistance to H₂O inhibition

As was mentioned in Introduction, an addition of Pt prolongs the lifetime of the PdO/Al₂O₃ catalyst [27–30,41]; and therefore, both monometallic Pt/Al₂O₃ and Pd/Al₂O₃, as well as a bimetallic PtPd/Al₂O₃ were examined. Temperature-programmed methane oxidation was performed with four sequential ramps (ramp 1: heating, ramp 2: cooling, ramp 3: heating, ramp 4: cooling) with 500 ppm CH₄, 8% O₂, and 5% H₂O as described in Experimental Section 2.2 (Fig. 1B). The resulting methane conversions are shown in Fig. 3. To simplify the figure, only ramps 3 and 4 are shown for the monometallic samples, which are shifted to higher temperature region than ramps 1 and 2 for the corresponding sample.

The conversion of methane depends on a number of ramps as seen in Fig. 3. It should be noted that without water in the gas feed, all four

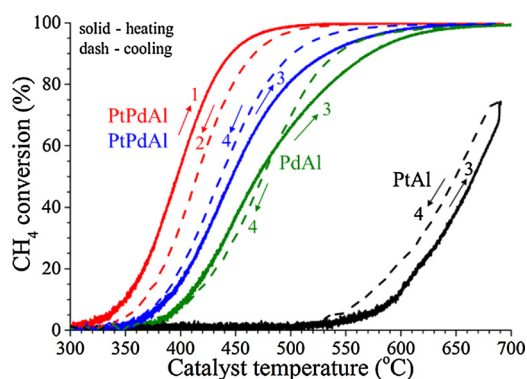


Fig. 3. Methane conversion versus temperature for the 1.9%Pt-3.8%Pd/Al₂O₃, 3.8%Pd/Al₂O₃ and 1.9%Pt/Al₂O₃ samples (WI) tested in methane oxidation (500 ppm CH₄; 8% O₂; 5% H₂O; Ar) under temperature-programmed conditions.

conversion curves stayed almost in the same position and did not shift to the higher temperature region, which is demonstrated in Fig. S1 (Supplementary material). The activity loss of the PtPd/Al₂O₃ sample during the ramping up and down is caused by the exposure to water and may be attributed to the continuous formation of –OH groups on the surface of support and on the active sites, which block active sites for methane adsorption [42–45]. The higher activity on ramp 4 compared to ramp 3 may be due to the fact that methane oxidation is an exothermic reaction. When monometallic Pd/Al₂O₃ and Pt/Al₂O₃ samples were tested under the same conditions as PtPd/Al₂O₃, it was observed that the Pt-based sample was active in methane oxidation at much higher temperature, which is similar to the literature reports [46,47]. Monometallic Pd/Al₂O₃ demonstrated much lower activity during ramps 3 and 4 than compared with bimetallic PtPd/Al₂O₃. The increased activity for PtPd/Al₂O₃ cannot be attributed to the increase in total noble metal loading since the amount of Pd was the same and Pt sites were not active at these low temperatures under lean conditions. Based on our earlier EDX analysis of bimetallic sample [38], PtPd alloys were formed, which was previously also observed in literature for PtPd-samples [48] and we suggest that it is this alloy formation that enhances the methane oxidation activity as seen in Fig. 3. Earlier, Weng et al. [49] hypothesized that PdO could play a key role under lean conditions, whereas metallic Pt could be catalytically active under rich conditions. In a recent study, Nassiri et al. [50] explained the improved performance of bimetallic PdPt-alloyed catalyst in the wet feed compared with methane oxidation activity of the monometallic Pd-only catalyst by the lack of oxygen on the surface for the PdPt-alloy, which allows Pt-catalyzed methane activation.

To summarize, enhanced activity of the bimetallic sample is owing to the fact that PtPd-alloys were formed, which may be more resistant to –OH formation and demonstrate different mechanism of methane oxidation than monometallic samples.

3.2. Resistance to SO₂-poisoning

The experiments at constant temperature were conducted in order to compare the resistance of the Pt-, Pd- and PtPd-based Al₂O₃ samples to SO₂ poisoning. Methane conversion was measured at the same temperature before and after the sulfur poisoning step which was conducted at lower temperatures to investigate the temperature effect on the stability of surface sulfates formed during the poisoning step. To facilitate the sulfur regeneration, the temperature before and after sulfation was chosen to be 550 °C, but the poisoning was performed at 500 °C. The results shown in Fig. 4 demonstrate the methane conversion

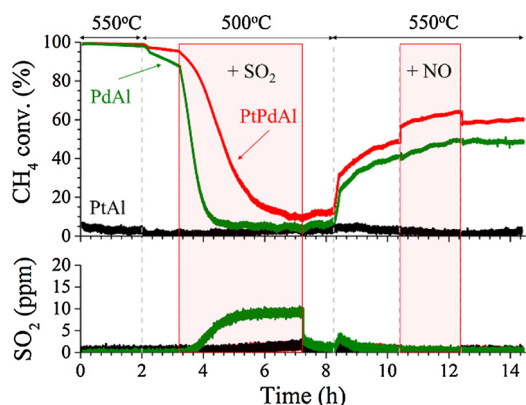


Fig. 4. Methane conversion (top panel) and outlet concentration of SO₂ (bottom panel) for the 1.9%Pt-3.8%Pd/Al₂O₃; 3.8%Pd/Al₂O₃ and 1.9%Pt/Al₂O₃ samples (batch WI). Gas composition: 500 ppm CH₄, 8 vol.% O₂, 5 vol.% H₂O in Ar unless otherwise specified; for SO₂-poisoning step: + 10 ppm SO₂ and for NO-containing step: + 500 ppm NO. The temperature is displayed in the figure.

levels obtained for the three samples (top panel) and the outlet concentration of SO₂ (bottom panel) during the length of the experiment.

The samples were treated for 2 h at 550 °C with the initial gas mixture; full CH₄ conversion was obtained on both samples that contain Pd, whereas Pt/Al₂O₃ sample remained inactive under the same conditions during the length of the experiment. It was shown in Fig. 3, that PtAl catalyst is active in methane oxidation at higher temperatures under lean conditions. Since the conversion reached 100% it is not possible to examine the H₂O resistance between Pd/Al₂O₃ and PtPd/Al₂O₃. Thereafter, the temperature was decreased to 500 °C, while the samples were treated with the same inlet gas mixture for 1 h. A clear difference in methane oxidation activity was observed. The rate of deactivation of Pd/Al₂O₃ exceeded the deactivation rate of PtPd/Al₂O₃ and after 1 h, 95% and 87% of methane conversion were achieved for PtPd/Al₂O₃ and Pd/Al₂O₃, respectively. The catalytic activity loss may be related to the formation of surface hydroxyl groups on the support, as well as on active sites [42–45] as was discussed in connection to the Fig. 3.

The sulfur resistance of the samples was tested by adding 10 ppm of SO₂ to the inlet gas mixture at 500 °C and samples were kept under the SO₂-containing gas mixture for 4 h. Afterwards, the flow of SO₂ was stopped and samples were treated with the inlet gas mixture for another hour without changing the temperature. This treatment was done to detect the deactivation during the SO₂-poisoning step by comparing conversion level of poisoned samples with the level obtained on non-poisoned samples. During the SO₂-poisoning step, a significant loss in catalytic activity on both samples was observed; however, the deactivation of the bimetallic sample occurred slower. For example, the methane conversion dropped from 87% to 10% within 1 h under the SO₂-containing gas mixture for Pd/Al₂O₃; but on the PtPd/Al₂O₃ sample, methane conversion slowly decreased from initial 95% to 66% after 1 h and still exhibited activity after 4 h (10%), which is seen in Fig. 4. Moreover, a clear difference in SO₂ outlet concentration during the catalytic activity tests could be detected. When the methane conversion reached a level of 10% on the Pd/Al₂O₃ sample, the SO₂ outlet concentration reached 4 ppm and after one more hour it reached the initial level of 10 ppm and stayed constant until SO₂ had been excluded from the reactant gas mixture. In the case of both Pt-containing samples, the SO₂ outlet level reached only 1–2 ppm at the end of the SO₂-poisoning step, despite the fact that the Pt/Al₂O₃ sample had not demonstrated any activity in methane oxidation. This observation suggests that Pt was active in SO₂ oxidation to form SO₃, which promote the formation of sulfates on alumina surface, which is in line with the study by Gandhi and Shelef [1]. PdO is capable to oxidize SO₂ to SO₃; however, it forms stable complex Pd-SO₄ which is less active in methane oxidation than PdO [4,21]. The higher resistance of PtPdAl sample to SO₂ may be due to that Pt in metallic state adsorbs SO₂ which prevents interaction of it with surface palladium oxide leading to lower deactivation rate in methane oxidation [12]. Another possibility is that in the presence of Pt, sulfates that occupy PdO active sites are more mobile and can migrate to alumina support. Although PtPd sample was more resistant to SO₂-poisoning than Pd-only sample, the reactivity of both catalysts could not be restored after the treatment under the reaction gas mixture without SO₂ at T = 500 °C.

The amount of SO₂ consumed during the poisoning step (relating to experiments in Fig. 4) are shown in Table 1, accompanied by methane conversions over Pd/Al₂O₃ and PtPd/Al₂O₃.

For the Pd/Al₂O₃ sample, the amount of SO₂ consumed after 4 h of poisoning step corresponds to the Pd loading in the sample. Moreover, most of the SO₂ (around 70% of total amount) was consumed during first two hours while catalytic activity dropped significantly from 87 to 6%, whereas for bimetallic sample conversion dropped from 95% to 28%. However, no SO₂ in outlet was detected during this experiment, resulting in that the amount of SO₂ consumed was significantly larger than the PtPd content in the sample. These results suggest that in the presence of Pt, the oxidation of SO₂ to SO₃ and H₂SO₄ formation are

Table 1

Amount of SO₂ (inlet, outlet, consumed, in mmol/g cat) during four hours poisoning step at 500 °C over Pd/Al₂O₃ and PtPd/Al₂O₃ (batch WI), accompanied by conversion of CH₄.

T = 500 °C	3.8 wt.% Pd/Al ₂ O ₃					1.9 wt.%-3.8 wt.% Pd/Al ₂ O ₃				
Metal loading	0.357 mmol/g cat					0.454 mmol/g cat				
Duration	0 h	1 h	2 h	3 h	4 h	0 h	1 h	2 h	3 h	4 h
CH ₄ conversion, %	87	11	6	5	3	95	68	28	13	9
SO ₂ in, mmol/g cat	—	0.226	0.453	0.679	0.906	—	0.226	0.453	0.679	0.906
SO ₂ out, mmol/g cat	—	0.035	0.194	0.393	0.600	—	0	0	0	0
SO ₂ consumed, mmol/g cat	—	0.191	0.258	0.286	0.306	—	0.226	0.453	0.679	0.906

Note: SO₂ amount is total after 1 h; after 2 h and so on.

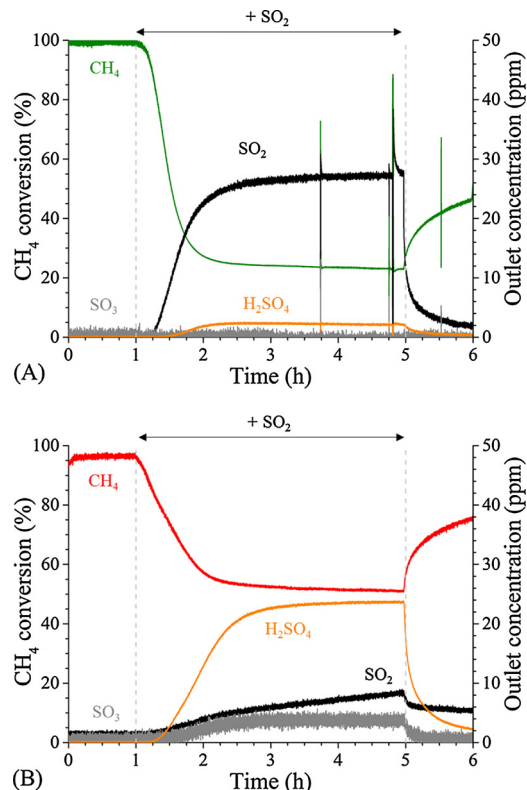


Fig. 5. Methane conversion and outlet concentration of SO₂, SO₃ and H₂SO₄ at 500 °C for the 3.8%Pd/Al₂O₃ (A) and 1.9%Pt-3.8%Pd/Al₂O₃ (B) samples (batch WI). Gas composition: 500 ppm CH₄, 8 vol.% O₂, 5 vol.% H₂O in Ar; for SO₂-poisoning step: + 30 ppm SO₂.

enhanced, which facilitates sulfur storage on the alumina as discussed above.

When the experiments were repeated on a new batch WI using the same reaction protocol as shown in Fig. 1C with higher concentration of SO₂, it was found that the WI batch (see Fig. 5) was more active than the previous WI batch. However, the results demonstrated the same trends, where PtPd/Al₂O₃ is significantly more active during the sulfur exposure compared to Pd/Al₂O₃. Thus, this beneficial effect of Pt addition is found using two different preparation methods for the catalyst. Moreover, outlet concentrations of SO₂, SO₃ and H₂SO₄ are shown in Fig. 5 accompanied by conversion of methane at 500 °C. It is obvious that PtPd/Al₂O₃ sample comparing to Pd/Al₂O₃ is capable to continuously oxidize SO₂ to SO₃, followed by formation of sulfuric acid due to high water content.

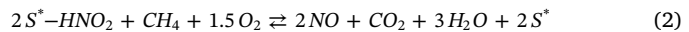
During the next step in Fig. 4, the temperature increased up to 550 °C under the inlet gas mixture which led to the partial re-establishment of catalytic activity. After six hours under the SO₂-free gas mixture, methane conversion reached only 49% and 60%, over Pd/Al₂O₃ and PtPd/Al₂O₃ catalysts, respectively, compared to close to

100% before the poisoning step. The gradual increase in methane conversion during this period could be attributed to the decomposition of surface sulfur species, which had been formed during the previous step at lower temperature. It is obvious that the efficiency of the regeneration increased with increasing the regeneration temperature. However, under lean conditions the complete regeneration of S-poisoned samples occurs only at temperatures above 750 °C after the decomposition of stable aluminum sulfates as concluded by Arosio et al. [51]. Several studies investigated regeneration procedures to regain catalytic activity of sulfur poisoned samples and mostly confirmed that reducing conditions led to decreased temperature of regeneration due to reduction of sulfates to SO₂; however, there is a possibility of formation of metal sulfides which are hard to remove [9,11,52,53].

It is interesting to note the effect of changing gas composition by the addition of NO to the inlet gas mixture (Fig. 4). An increase by 10% in methane conversion was observed over the PtPd/Al₂O₃ sample, whereas no noticeable effect was achieved on Pd/Al₂O₃. In our earlier work [38], we proposed that one of the beneficial effects with NO was the removal of hydroxyl groups from the active sites to possibly form HNO₂ species, which are very active:



where S* is the active site. The HNO₂ species could thereafter help to activate the methane [38]. Since there is no overall consumption of NO_x, it indicates that NO is being formed from the reaction with HNO₂ and a possible overall reaction for this is



Pt-containing material is a powerful catalyst for oxidation reactions, and that could be the reason for that the beneficial effect of NO is only observed in the presence of Pt and not on Pd/Al₂O₃ alone. However, the NO positive effect was considered temporary and could be observed only when NO was co-fed to the reaction gas mixture, which can be explained by the two reactions above. When NO was excluded from the inlet gas flow, methane conversion dropped down by 10%. Moreover, methane conversion over both samples reached steady-state level after the NO-containing step. These results are in line with the work by Oktar et al. [54], that observed based on infra-red spectroscopy that NO_x reduction proceeds through the interaction of CH₄ with surface bidentate nitrates. In our experiments we use excess of water (5%) and we therefore suggest a mechanism here based on reactive -HNO₂ species.

Based on the results shown in Fig. 4, it can be concluded that Pd- and PtPd-containing samples are deactivated under SO₂-containing gas flow, but the bimetallic sample could withstand the deactivation better. It is also demonstrated that catalysts can be partly regenerated with the initial gas mixture under lean conditions at the higher temperature than that used for SO₂-poisoning step and that the PtPd-containing sample possessed higher activity also after the reaction step without sulfur compared with Pd/Al₂O₃.

To regenerate the catalytic activity, the samples were treated under different regeneration conditions at 550 °C. In Fig. 6, the results of methane conversion obtained after regeneration procedures under inert or reducing conditions can be compared.

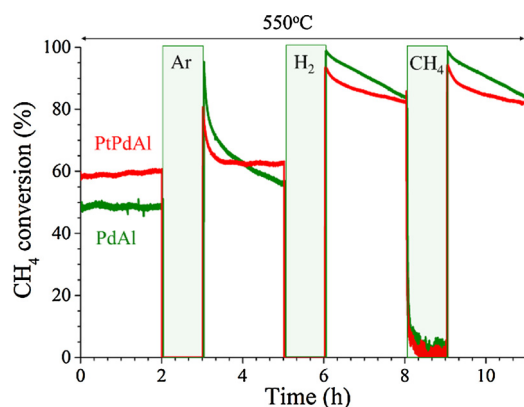


Fig. 6. Effect of gas composition on activity of S-poisoned 1.9%Pt-3.8%Pd/Al₂O₃ and 3.8%Pd/Al₂O₃ samples measured at 550 °C using the initial gas composition of 500 ppm CH₄, 8 vol.% O₂, 5 vol.% H₂O in Ar; for Ar regeneration: Ar flow; for H₂ regeneration: 2000 ppm H₂, Ar; for CH₄ regeneration: 500 ppm CH₄, Ar.

Initially, the methane conversion level of two S-poisoned samples reached 60% and 49% at 550 °C on PtPd/Al₂O₃ and Pd/Al₂O₃, respectively. Under two hours of experiments, the conversion demonstrated steady-state level. Thereafter, the samples were treated under inert Ar flow at the same temperature for 1 h. When samples were again exposed to the initial gas mixture after the regeneration step in Ar, the methane conversion level reached 63% on PtPd/Al₂O₃ and 55% on Pd/Al₂O₃ at the end of the 2-hour step, but the conversion was still decreasing especially for Pd/Al₂O₃. Our observations show that PtPd/Al₂O₃ is more active than Pd/Al₂O₃ and is deactivated more slowly by sulfur dioxide (see Fig. 4), which is in line with results reported by several groups [12,29,37,53]. These results suggest that PtPd/Al₂O₃ is more resistant to sulfur poisoning due to the function of the Pt additive and possess a slower decrease in methane conversion. Moreover, during the Ar step, the surface –OH groups partly decomposed and re-formed again during the methane oxidation in the presence of water, which resulted in a decrease of methane conversion during the step after the Ar regeneration. However, the decrease in methane conversion over the samples is significantly faster after sulfur poisoning compared with non-poisoned samples, for example, before poisoning the conversion over PdAl was almost 100% at 550 °C for two hours, whereas during the same time after sulfur poisoning a decrease in methane conversion from 84% to 56% was observed. Sulfur poisoning in dry conditions was also conducted over one PtPd/Al₂O₃ sample and the results presented in Fig. 7 clearly show that there is only a minor deactivation by SO₂ when using a dry reaction gas mixture. It can therefore be concluded that

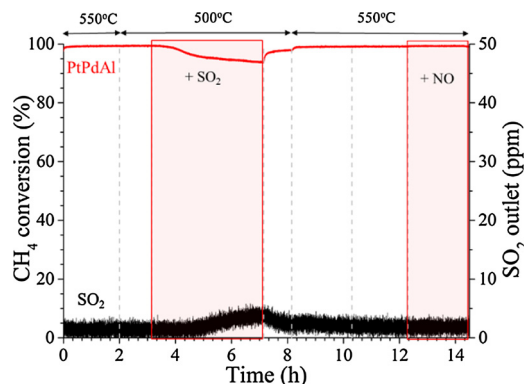


Fig. 7. Methane conversion and outlet concentration of SO₂ obtained over the 1.9%Pt-3.8%Pd/Al₂O₃ in methane oxidation under dry conditions. Gas composition: 500 ppm CH₄, 8 vol.% O₂ in Ar; + 500 ppm NO if added; + 10 ppm SO₂ if added.

moist condition facilitates inhibition caused by SO₂. This observation agrees well with the finding that the S-poisoned catalyst is more sensitive to water inhibition compared to the fresh samples [26,33]. The obtained results in Fig. 6 indicate that the sulfur remaining on the catalyst interacts with the hydroxyl species formed during the treatment with wet feed.

After the regeneration under reducing conditions (H₂ in Ar), the activity of both samples shown in Fig. 6 was significantly improved, which is in line with earlier studies [9,11,51–53]. When samples were treated under CH₄ flow, the same conversion level was observed compared with the treatment in H₂ flow. No difference in H₂ or CH₄-containing flow on the methane conversion level was detected; however, it should be noted that the reverse order of treatment may reveal other results. The reduction step facilitated sulfates removal from both samples, however, the methane conversion still decreased faster after the methane step compared to the case for the fresh catalyst. These results suggest that a part of the S-containing surface species still stayed on catalysts, which is discussed below in connection to the XPS and TEM-EDX results.

XPS measurements were conducted over the sulfur regenerated catalysts (see Fig. 6), and the results are shown in Fig. 8. It is clear that residual sulfur species are present in form of sulfates with a maximum of 169.8 eV binding energy obtained for the three samples PtPd/Al₂O₃, Pd/Al₂O₃, and Pt/Al₂O₃. No shift of binding energy in the sulfates region (169–171 eV) [55] was observed for the three samples. The residual sulfates prevent the activity to be fully regained at these temperatures as could be seen in Fig. 6. To reach full regeneration, higher temperatures are most likely required, for example, 600 °C and higher, which is also demonstrated in the literature [51,52].

To detect where the sulfates are located on the surface, the powder was taken from the monoliths after regeneration and was then used in TEM measurement accompanied by the EDX analysis. The results in Fig. 9 show that even after catalytic activity tests and the SO₂-poisoning step followed by regeneration, the PtPd/Al₂O₃ sample demonstrated similar particle sizes as for non-sulfated samples (about 15 nm). For the sulfur treated sample the average size of nanoparticles was approx. 11 nm with the presence of bigger particles at 20 nm, as well as smaller at 5 nm as shown in Fig. 10, which demonstrates the particle size distribution. The dispersion of noble metals based on the average size was 11% counted based on the STEM results and using the correlation for dispersion found in [39,40]. To summarize, the noble metal sintering was not responsible for the lower activity after the sulfur poisoning and regeneration since the dispersion was not decreased.

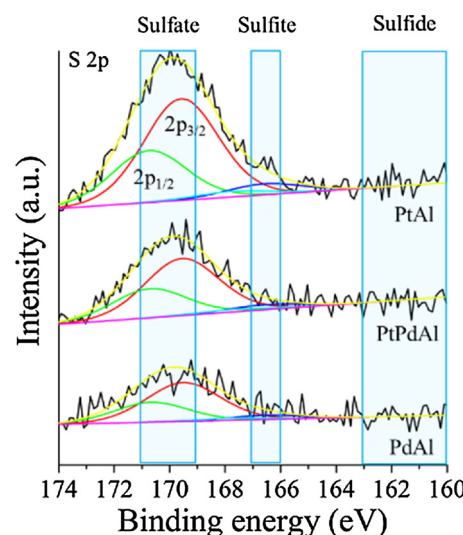


Fig. 8. S 2p core level spectra from XPS measurements, recorded on three SO₂-poisoned samples after their regeneration (shown in Fig. 6).

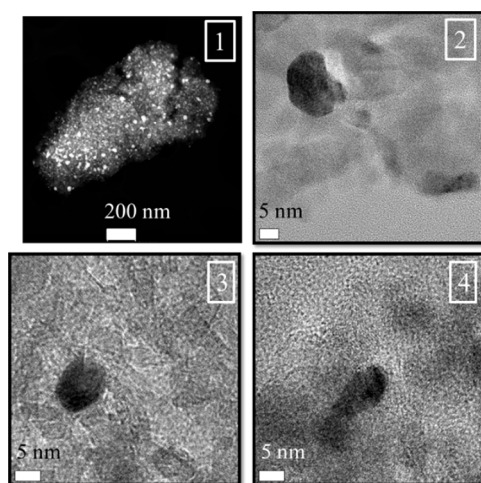


Fig. 9. TEM images of the SO_2 -poisoned 1.9%Pt-3.8%Pd/ Al_2O_3 sample after the regeneration procedures.

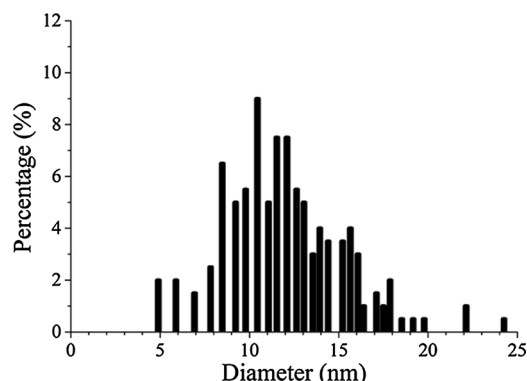


Fig. 10. Particle size distribution over the SO_2 -poisoned 1.9%Pt-3.8%Pd/ Al_2O_3 sample after the regeneration procedures based on 200 particles counting.

As shown in Fig. 11 from the EDX analysis, both Pt and Pd are present in the whole particles, which suggest alloy formation, but also that there are platinum enriched spots. Moreover, the EDX-mapping shows that the sulfur is concentrated to the noble metal particles. Interestingly, the platinum enriched areas of the particles contain additional amount of sulfur which is shown by the higher brightness in the Pt-rich areas. In order to confirm these results, EDX-mapping has also been performed on other particles (see Fig. S2, A and B), where the same observations were found. This finding confirms that the formation of PtPd alloys promotes the SO_2 adsorption on metallic Pt, which thereby lowers the formation of sulfates on palladium oxide.

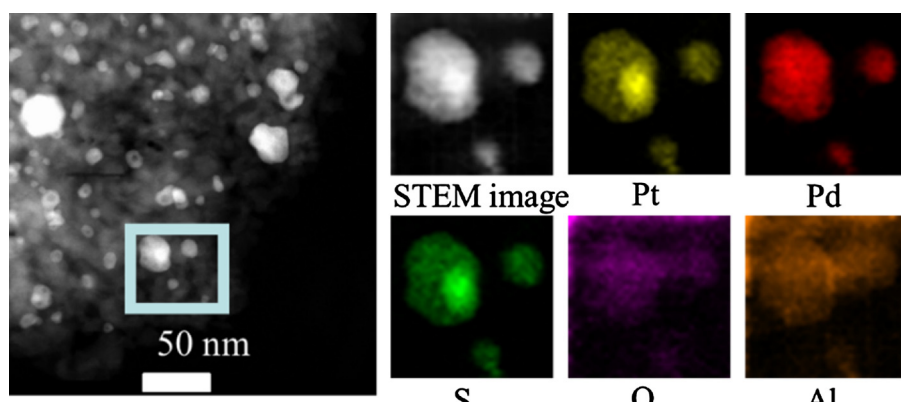


Fig. 11. STEM image and EDX-mapping of the 1.9 wt.%Pt-3.8 wt.%Pd/ Al_2O_3 sample after the regeneration procedures.

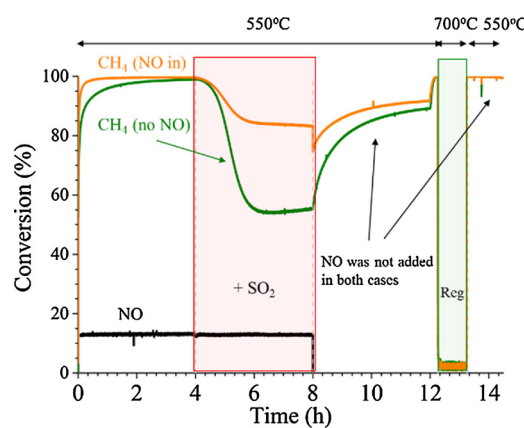


Fig. 12. Methane and NO to NO_2 (black) conversion obtained on two different 1.9%Pt-3.8%Pd/ Al_2O_3 catalysts (batch WI) at 550 °C followed by the reduction in 500 ppm CH_4 in Ar flow at 700 °C. Initial gas composition: 500 ppm CH_4 , 8 vol.% O_2 , 5 vol.% H_2O in Ar (green) and 500 ppm NO added only at first two steps 0–8 h (orange); for SO_2 -poisoning step: + 10 ppm SO_2 . Note the sample that was not exposed to NO was cooled in Ar flow only after the pre-treatment (For interpretation of the references to colour in this figure legend, the reader is referred to the web version of this article).

To summarize, the bimetallic PtPd/ Al_2O_3 sample is more resistant towards sulfur poisoning compared to monometallic Pd/ Al_2O_3 . Moreover, water significantly increased the poisoning effect. The regeneration of SO_2 -poisoned samples could be performed partly under either lean or rich conditions at 550 °C, but with higher efficiency under reducing conditions. Residual sulfur observed in the form of sulfates was still present on the catalyst surface after reduction at 550 °C. The sulfur was concentrated to the noble metal particles, and significantly enriched to the Pt rich parts, which might protect the palladium from sulfur and thereby explain the slower poisoning on the bimetallic catalyst.

3.3. NO effect on resistance to SO_2 -poisoning

Several types of activity tests were conducted in order to investigate SO_2 -poisoning in detail and as described in the Experimental Section 2.2, a new monolith was tested for each sulfur experiment in order to ensure the sulfate-free surfaces for the comparison purposes.

Fig. 12 demonstrates differences in CH_4 conversion observed while testing PtPd/ Al_2O_3 in methane oxidation with (orange) and without (green) additional NO at 550 °C. Conversion of NO to NO_2 in the case when initial gas mixture contained NO is also present on in Fig. 12. Although after first four hours, both samples reached 100% CH_4 conversion, one can notice the differences in methane conversion during the first two hours of the experiment.

For NO-free gas mixture CH_4 conversion started at 85% and continued increasing with time; in the case of NO-containing gas mixture the conversion level reached 100% within 20 min. Nitrogen dioxide was formed and resulted in an NO conversion of about 13%. After the sample had been poisoned in the SO_2 -containing flow for the next four hours the sulfur inhibition became noticeable. Comparing with the results of PtPdAl sample poisoned at 500 °C (Fig. 4), the SO_2 -poisoning at 550 °C is less severe, which is in line with the reports [9,53] demonstrated that the extent of SO_2 -poisoning depends on poisoning temperature. As noticed, the conversion obtained on two samples during the SO_2 -poisoning step reached varying steady-state levels. Conversion of 85% was reached when NO had been included in the gas mixture, whereas only 55% was demonstrated in the case of the NO-free gas flow. At the same time, no noticeable effect of SO_2 addition on NO conversion was observed. It should be noted that total NO_x was constant in all experiments and the NO conversion was only to produce NO_2 . It is clear that in the presence of NO, the rate of deactivation by SO_2 was decreased. Moreover, when both samples had been treated in the NO-free gas mixture afterwards, the sample that previously had been treated with NO exhibited higher activity, but the difference between the samples decreased with time. However, in the end of the step, only about 90% CH_4 conversion was reached on both samples, compared to full conversion before sulfur treatment. These results show that there is still sulfur remaining on the active sites, which reduces the methane conversion. After the regeneration under reducing conditions at 700 °C, both samples demonstrated full conversion levels at 550 °C as shown before the SO_2 -poisoning step. It is important to note that there is still likely sulfur remaining on the catalyst as was the case for the sulfur poisoning at 500 °C, but it cannot be observed at this higher temperature due to that the sample reaches full conversion.

Fig. 13 demonstrates the activity of the PtPd/Al₂O₃ sample during alternate steps in SO_2 -containing flow and reduction by CH_4 . The difference between the two experiments was in the addition of NO to the inlet gas mixture. One sample was treated in the presence of NO from the beginning of the experiment and during all methane oxidation steps (orange line). Methane conversion over this sample is accompanied by conversion of NO to NO_2 . Another sample was initially treated without NO during the first four hours; however, then NO was added to the gas flow. Note that during methane regeneration only methane in Ar was present, i.e. no NO was added for both samples. Already during the first SO_2 -containing step, a difference in the methane conversion was observed between two samples. This difference increased drastically during the second SO_2 -containing step, where for the catalyst without

NO, the conversion dropped to 75%; however, in the presence of NO, it only dropped to 90%. For the two last sulfur poisoning steps, both experiments contained NO and it is clear that very similar results were obtained. These results clearly show that the presence of NO during sulfur poisoning lowers the poisoning effect.

In order to further study the regeneration effect, an experiment was conducted where the activity was examined at lower temperature, where conversion was not reaching 100%. These experiments were performed on the catalyst prepared by IWI and the results are shown in Fig. S3 in Supplementary material, together with a detailed description of the experimental procedure. Firstly, it is found that the IWI prepared catalyst has higher activity, as previously mentioned. Moreover, in these experiments, the catalyst was first exposed to reaction conditions only for 2 h at 550 °C, which was followed by lowering the temperature to 400 °C. At this lower temperature, the experiment with NO actually resulted in an inhibition, which was also found in one of our earlier studies [39]. During sulfur poisoning at 550 °C, the sulfur poisoning was again inhibited by NO, resulting in higher activity with NO. However, the effect was smaller compared to the results shown in Fig. 12 and the reason for this could be both that the IWI batch is more active and that the catalyst was only exposed to the gas mixture for 2 h at 550 °C, compared to 4 h, which likely results in less hydroxyl species on the active sites. Moreover, it is clear that even after the regeneration under rich conditions at 700 °C, the catalyst did not regain the same activity at 400 °C.

The NO effect on SO_2 -poisoning was also studied at a lower temperature (450 °C). Two samples of PtPd/Al₂O₃ (the same batch WI) were treated under the initial gas mixture during ten hours each. Fig. 14 demonstrates the CH_4 conversion accompanied by the NO to NO_2 conversion (black) obtained during the above mentioned experiments. In the case when NO was absent from the gas mixture, methane conversion declined faster (green) compared to the case when NO was co-fed to the reaction mixture (orange). The decrease in CH_4 conversion is explained by the continuous hydroxylation of support and active sites. Conversion NO to NO_2 reached 28% and stayed at the same level for 10 h. Neither N_2O formation nor NO_x reduction during this step were observed. This difference may arise from the fact that NO facilitates methane oxidation by the reaction with surface hydroxyls to form HNO_2 as was suggested in our previous study [38]. After 10 h, SO_2 was introduced to the gas mixture and conversion continuously decreased on both samples; however, in the case of NO presence, the steady-state value of methane conversion was 13% compared to the 8% obtained without NO. Thus, also at this temperature the addition of NO results in higher methane conversion during sulfur poisoning. It should be noted

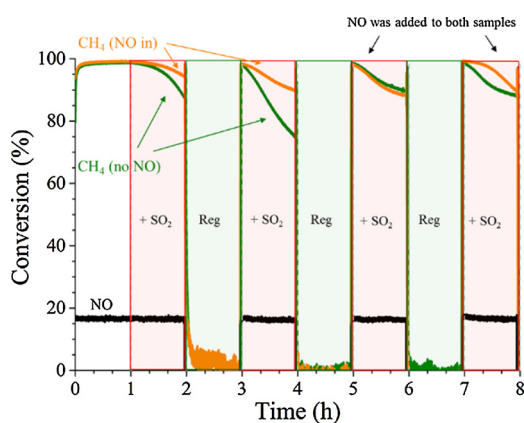


Fig. 13. Methane and NO (to NO_2) conversion obtained on two different 1.9% Pt-3.8%Pd/Al₂O₃ catalysts (same batch WI) at 550 °C followed by SO_2 -poisoning and CH_4 reduction at the same temperature. Initial gas composition: 500 ppm CH_4 , 8 vol.% O_2 , 5 vol.% H_2O in Ar (green) and 500 ppm NO if added (orange); for SO_2 -poisoning step: + 10 ppm SO_2 ; for CH_4 regeneration: 500 ppm CH_4 , Ar (For interpretation of the references to colour in this figure legend, the reader is referred to the web version of this article).

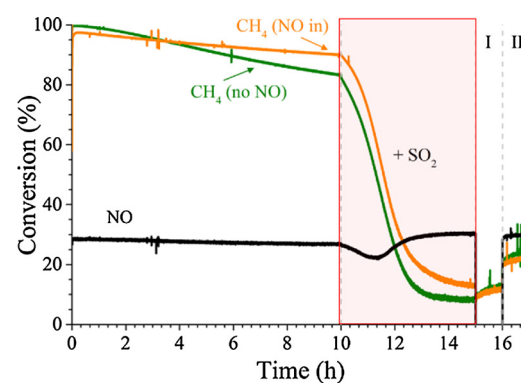


Fig. 14. Effect of NO on methane conversion measured on two different 1.9% Pt-3.8%Pd/Al₂O₃ catalysts (batch WI) at 450 °C. Initial gas composition: 500 ppm CH_4 , 8 vol.% O_2 , 5 vol.% H_2O in Ar (green) and 500 ppm NO if added (orange); for SO_2 -poisoning step: + 10 ppm SO_2 ; for step I: initial gas composition for both samples; for step II: + 500 ppm NO for both samples (For interpretation of the references to colour in this figure legend, the reader is referred to the web version of this article).

that at the same time as SO_2 was added, the NO conversion decreased by 6%; which occurred simultaneously with a decrease in the temperature of 7 °C (see Figure S4), due to lower exotherm from the reduced methane oxidation. However, after reaching a minimum value, it increased again and exceeded the initial level obtained on non-poisoned samples. The same effect was slightly observed at 500 °C (only 1% drop of NO conversion); however, at 550 °C no effect on NO conversion was detected. The reason for this decrease in NO conversion could be that since the sulfates are more thermodynamic stable species than nitrates [56] and displace nitrates on the catalyst surface, which may lower NO conversion. After SO_2 removal, both samples demonstrated a similar methane conversion of 12% with an increase of up to 23% in the presence of NO.

As shown by the activity tests performed at various temperatures, continuous presence of NO in a feed delays the inhibition of the PtPd/ Al_2O_3 sample caused by SO_2 and H_2O ; however, the effect greatly depends on the temperature of SO_2 exposure.

Infra-red spectroscopy was used to detect surface species formed at 500 °C during the exposure of the samples to SO_2 -containing initial gas mixture in the absence and presence of NO. The pretreatment procedures of the samples are described in detail in Experimental Section 2.3. Prior to spectra recording, the samples were exposed to SO_2 -containing gas mixture at 450 °C to partly deactivate samples and form highly stable surface sulfates on Al_2O_3 . Experiments were also performed without this pre-treatment with SO_2 (not shown here), but no effect of NO was seen, likely due to the large build-up of sulfates on the support.

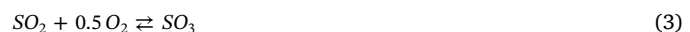
The spectra displayed in Fig. 15 at 1400–900 cm^{-1} were recorded every five minutes and show the difference in the intensity of bands developing under SO_2 -containing gas flow, which were attributed to various types of surface S-containing species.

First, the sample treated without NO (Fig. 15A) exhibited a growth of two major bands at 1191 cm^{-1} and 1054 cm^{-1} . During the first 10 min, these main bands remained, which then were accompanied by the increase in intensity of left and right shoulders at 1273 cm^{-1} and 1019 cm^{-1} , respectively. According to literature the band at 1191 cm^{-1} with a broad shoulder at 1273 cm^{-1} is a characteristic band of bulk aluminum sulfates [21,42,57,58]. A broad band appeared at 1054 cm^{-1} with a shoulder at 1019 cm^{-1} may be attributed to surface sulfates on alumina [58] or surface aluminum sulfites [57,59]. Then after 10 min, the band at 1106 cm^{-1} appeared and continued to grow during the whole experiment in contrast to the intensity of 1191 cm^{-1}

and 1054 cm^{-1} which did not change much during the last 20 min of the experiment suggesting the saturation of the sample. Bulk PdSO_4 resulted in peaks at 1240 cm^{-1} and 1100 cm^{-1} [21], however, the band at 1106 cm^{-1} may be assigned to aluminum surface sulfites [11,60]. To conclude upon the exposure of PtPdAl sample with SO_2 -containing gas flow, the formation of bulk alumina sulfates (1191 and 1273 cm^{-1}) and surface sulfates (1054 and 1019 cm^{-1}) occurred. No traces of bulk PdSO_4 formation (1240 and 1100 cm^{-1}) was detected; however, it may be due to the pre-poisoned conditions of the samples. When sulfates were formed, surface sulfites appeared (1106 cm^{-1}).

In the presence of NO (Fig. 15B), the same bands development was observed, however, with different intensity. Less intensive bands were observed for bulk aluminum sulfates (1273 and 1191 cm^{-1}) and for surface aluminum sulfates (1054 and 1019 cm^{-1}). The band at 1106 cm^{-1} was much more intense in the case of NO presence and was attributed to surface sulfite formation [60]. Fig. 16 demonstrates differences in the intensity of two major bands assigned to the bulk aluminum sulfates (1191 cm^{-1}) and surface sulfites (1106 cm^{-1}) when sample was treated without (A) and with (B) NO in a gas mixture. It is clear that addition of NO hindered sulfates accumulation and favored formation of sulfites.

Based on the combined flow reactor and *in-situ* DRIFT spectroscopy we propose a mechanism below for the NO impact on the sulfur poisoning. First, it was clear from the experiment shown in Fig. 7, that the sulfur poisoning is significantly less without water. This means that the water plays an important role for the poisoning and this can be described in the following two steps



where S^* is the active site.

These reactions are in line with the DRIFT spectroscopy results where sulfates were detected. However, in the presence of NO, the NO could react with the $-\text{OH}$ groups to form HNO_2 (see Eq. (1)), that can activate methane (See Eq. (2)). Since $-\text{OH}$ groups are being removed from the surface by the NO, the rate of Eq. (4), where the sulfates are formed, will be reduced and instead the sulfites are favored. In addition, for the experiment conducted at 450 °C (Fig. 14), there is actually an increased NO_2 formation, when comparing the later part of the sulfur step. This may be explained by the reaction of NO with sulfates to form sulfites and NO_2 ; however, no NO_2 in a gas phase was detected by

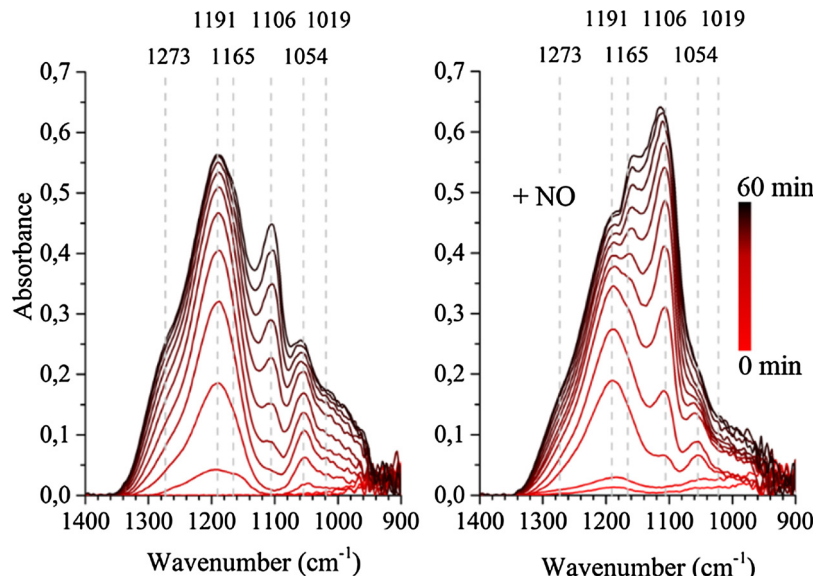


Fig. 15. DRIFT spectra collected at 500 °C every 5 min on the powder 1.9%Pt-3.8%Pd/ Al_2O_3 samples (the same batch WI) in the absence (left) and presence (right) of NO in a reaction gas mixture consisting 1000 ppm CH_4 , 1.5 vol.% O_2 , 1 vol.% H_2O , 500 ppm SO_2 in Ar and 1000 ppm NO if added.

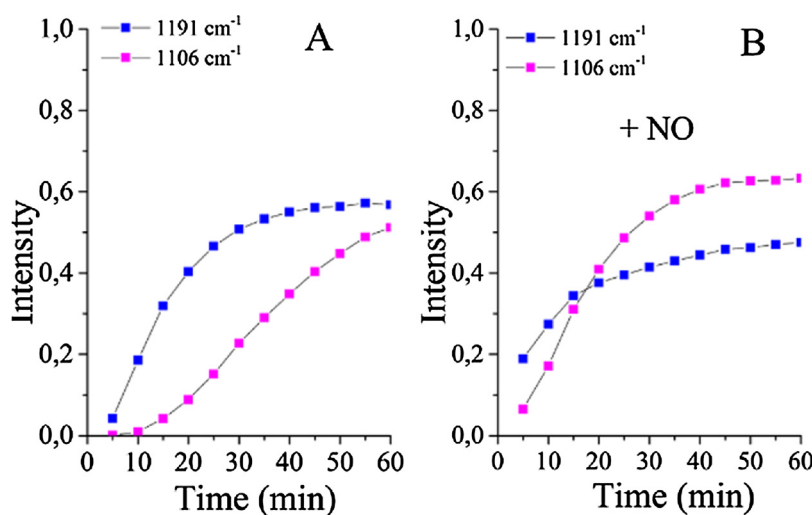


Fig. 16. DRIFT spectra collected at 500 °C every 5 min on the powder 1.9%Pt-3.8%Pd/Al₂O₃ samples (same batch WI) in the absence (left) and presence (right) of NO in a reaction gas mixture consisting 1000 ppm CH₄, 1.5 vol.% O₂, 1 vol.% H₂O, 500 ppm SO₂ in Ar and 1000 ppm NO if added.

infra-red spectroscopy.

As a conclusion, the presence of NO lowers the sulfate formation and mostly surface sulfites are observed, which increases the lifetime of the catalyst during SO₂ exposure.

4. Conclusion

In this study, the bimetallic PtPd/Al₂O₃ sample was investigated in complete methane oxidation using various gas compositions and the activity was compared to the activity of monometallic Pd/Al₂O₃ and Pt/Al₂O₃. Enhanced activity of the bimetallic sample obtained during experiments with wet feed is owing to the fact that PtPd-alloys were formed, which may be more resistant to –OH formation and demonstrate different mechanism of methane oxidation than monometallic samples under the same conditions.

Both Pd- and PtPd-containing samples are deactivated under SO₂-containing gas flow, but the bimetallic sample could withstand the deactivation during prolonged periods. Since only a minor deactivation by SO₂ was demonstrated in the experiments performed without water in the reaction gas mixture, it was concluded that moist condition facilitates inhibition caused by SO₂. The relation between the temperature of SO₂-poisoning step and the extent of the deactivation was also studied; at the lower temperature the greater deactivation was observed. Regeneration of the poisoned samples could be partly performed under lean conditions at higher temperature than that used for SO₂-poisoning step and the PtPd-containing sample possessed higher activity compared with Pd/Al₂O₃. Moreover, the samples could be more effectively regenerated under reducing condition. As shown by XPS and TEM-EDX data, after reduction at 550 °C of the poisoned sample, residual sulfur remained on the surface in the form of sulfates, which were difficult to decompose and much higher temperature of regeneration is likely required. Moreover, the TEM and EDX mapping showed that sulfur was present in the whole noble metal particle, but significantly enriched in the Pt rich locations. The enrichment of sulfates to the platinum could result in partly protecting the palladium sites and could be the reason for slower sulfur deactivation of the bimetallic catalyst.

The flow reactor activity tests performed at various temperatures demonstrated that NO significantly delays the inhibition of the catalytic activity of PtPd/Al₂O₃ by SO₂ in the presence of water. However, the effect seems to be temporary and is significant if NO is constantly present in the gas mixture with SO₂ and H₂O. It was also noticed from the experimental results that the NO effect depends on the temperature and is the largest at temperatures close to 550 °C.

Both constant temperature experiments and DRIFTS results suggested that the formation of sulfates⁻ may explain the lower activity in complete methane oxidation in the presence of SO₂. However, in the presence of NO, a decrease of the sulfates and an increase of surface sulfites were observed by IR spectroscopy. The result of this study clearly demonstrates that including NO in the reaction mixture during methane oxidation slows down the rate of inhibition of the catalyst and increases lifetime, by reducing the amount of sulfates.

The findings of this study are of high practical interest due to the fact that H₂O, SO₂ and NO often are present in the exhaust and the presence of NO is a benefit both for the catalytic activity and also prolongs the catalyst lifetime due to the postponed sulfur inhibition.

Acknowledgments

This project is a collaboration between AVL MTC Motortestcenter AB, Johnson Matthey AB, Scania CV AB and Chalmers University of Technology. Swedish Energy Agency (FFI 37179-2) is gratefully acknowledged for its financial support.

Appendix A. Supplementary data

Supplementary material related to this article can be found, in the online version, at doi:<https://doi.org/10.1016/j.apcatb.2018.05.018>.

References

- [1] H.S. Gandhi, M. Shelef, Effects of sulfur on noble metal automotive catalysts, *Appl. Catal.* 77 (1991) 175–186, [http://dx.doi.org/10.1016/0166-9834\(91\)80063-3](http://dx.doi.org/10.1016/0166-9834(91)80063-3).
- [2] M.V. Twigg, Progress and future challenges in controlling automotive exhaust gas emissions, *Appl. Catal. B Environ.* 70 (2007) 2–15, <http://dx.doi.org/10.1016/j.apcatb.2006.02.029>.
- [3] M.V. Twigg, Catalytic control of emissions from cars, *Catal. Today* 163 (2011) 33–41, <http://dx.doi.org/10.1016/j.cattod.2010.12.044>.
- [4] J.K. Lampert, M.S. Kazi, R.J. Farrauto, Palladium catalyst performance for methane emissions abatement from lean burn natural gas vehicles, *Appl. Catal. B Environ.* 14 (1997) 211–223, [http://dx.doi.org/10.1016/S0926-3373\(97\)00024-6](http://dx.doi.org/10.1016/S0926-3373(97)00024-6).
- [5] P. Gélin, M. Primet, Complete oxidation of methane at low temperature over noble metal based catalysts: a review, *Appl. Catal. B Environ.* 39 (2002) 1–37, [http://dx.doi.org/10.1016/S0926-3373\(02\)00076-0](http://dx.doi.org/10.1016/S0926-3373(02)00076-0).
- [6] J.M. Jones, V.A. Dupont, R. Brydson, D.J. Fullerton, N.S. Nasri, A.B. Ross, A.V.K. Westwood, Sulphur poisoning and regeneration of precious metal catalysed methane combustion, *Catal. Today* 81 (2003) 589–601, [http://dx.doi.org/10.1016/S0920-5861\(03\)00157-3](http://dx.doi.org/10.1016/S0920-5861(03)00157-3).
- [7] A. Raj, Methane emission control, *Johns Matthey Technol. Rev.* 60 (2016) 228–235, <http://dx.doi.org/10.1595/205651316X692554>.
- [8] J.L. Aluha, G. Patrick, E. van der Lingen, Palladium-based catalysts with improved sulphur tolerance for diesel-engine exhaust systems, *Top. Catal.* 52 (2009) 1977–1982, <http://dx.doi.org/10.1007/s11244-009-9373-3>.
- [9] S. Ordóñez, P. Hurtado, F.V. Díez, Methane catalytic combustion over Pd/Al₂O₃ in

- presence of sulphur dioxide: development of a regeneration procedure, *Catal. Lett.* 100 (2005) 27–34, <http://dx.doi.org/10.1007/s10562-004-3081-1>.
- [10] L.S. Escandón, S. Ordóñez, A. Vega, F.V. Díez, Sulphur poisoning of palladium catalysts used for methane combustion: effect of the support, *J. Hazard. Mater.* 153 (2008) 742–750, <http://dx.doi.org/10.1016/j.jhazmat.2007.09.017>.
- [11] M.S. Wilburn, W.S. Epling, Sulfur deactivation and regeneration of mono- and bi-metallic Pd-Pt methane oxidation catalysts, *Appl. Catal. B Environ.* 206 (2017) 589–598, <http://dx.doi.org/10.1016/j.apcatb.2017.01.050>.
- [12] G. Corro, C. Cano, J.L.G. Fierro, A study of Pt-Pd/ γ -Al₂O₃ catalysts for methane oxidation resistant to deactivation by sulfur poisoning, *J. Mol. Catal. Chem.* 315 (2010) 35–42, <http://dx.doi.org/10.1016/j.molcata.2009.08.023>.
- [13] M. Monai, T. Montini, M. Melchionna, T. Duchoň, P. Kúš, C. Chen, N. Tsud, L. Nasi, K.C. Prince, K. Veltruská, V. Matolín, M.M. Khader, R.J. Gorte, P. Fornasiero, The effect of sulfur dioxide on the activity of hierarchical Pd-based catalysts in methane combustion, *Appl. Catal. B Environ.* 202 (2017) 72–83, <http://dx.doi.org/10.1016/j.apcatb.2016.09.016>.
- [14] A.W. Petrov, D. Ferri, M. Tarik, O. Kröcher, J.A. van Bokhoven, Deactivation aspects of methane oxidation catalysts based on palladium and ZSM-5, *Top. Catal.* 60 (2017) 123–130, <http://dx.doi.org/10.1007/s11244-016-0724-6>.
- [15] P. Gélin, L. Urfels, M. Primet, E. Tena, Complete oxidation of methane at low temperature over Pt and Pd catalysts for the abatement of lean-burn natural gas fuelled vehicles emissions: influence of water and sulphur containing compounds, *Catal. Today* 83 (2003) 45–57, [http://dx.doi.org/10.1016/S0920-5861\(03\)00215-3](http://dx.doi.org/10.1016/S0920-5861(03)00215-3).
- [16] Y.-H. Cathy Chin, M. García-Díéguez, E. Iglesia, Dynamics and thermodynamics of Pd-PdO phase transitions: effects of Pd cluster size and kinetic implications for catalytic methane combustion, *J. Phys. Chem. C* 120 (2016) 1446–1460, <http://dx.doi.org/10.1021/acs.jpcc.5b06677>.
- [17] S. Colussi, A. Trovarelli, G. Groppi, J. Llorca, The effect of CeO₂ on the dynamics of Pd-PdO transformation over Pd/Al₂O₃ combustion catalysts, *Catal. Commun.* 8 (2007) 1263–1266, <http://dx.doi.org/10.1016/j.catcom.2006.11.020>.
- [18] A.K. Datye, J. Bravo, T.R. Nelson, P. Atanasova, M. Lyubovsky, L. Pfefferle, Catalyst microstructure and methane oxidation reactivity during the Pd↔PdO transformation on alumina supports, *Appl. Catal. Gen.* 198 (2000) 179–196, [http://dx.doi.org/10.1016/S0926-860X\(99\)00512-8](http://dx.doi.org/10.1016/S0926-860X(99)00512-8).
- [19] J. Keating, G. Sankar, T.I. Hyde, S. Kohara, K. Ohara, Elucidation of structure and nature of the PdO-Pd transformation using *in situ* PDF and XAS techniques, *Phys. Chem. Chem. Phys.* 15 (2013) 8555–8565, <http://dx.doi.org/10.1039/c3cp50600b>.
- [20] S.K. Matam, G.L. Chiarello, Y. Lu, A. Weidenkaff, D. Ferri, PdO_x/Pd at work in a model three-way catalyst for methane abatement monitored by *operando* XANES, *Top. Catal.* 56 (2013) 239–242, <http://dx.doi.org/10.1007/s11244-013-9960-1>.
- [21] D.L. Mowery, R.L. McCormick, Deactivation of alumina supported and unsupported PdO methane oxidation catalyst: the effect of water on sulfate poisoning, *Appl. Catal. B Environ.* 34 (2001) 287–297, [http://dx.doi.org/10.1016/S0926-3373\(01\)00222-3](http://dx.doi.org/10.1016/S0926-3373(01)00222-3).
- [22] F. Ortloff, J. Bohnau, U. Kramar, F. Graf, T. Kolb, Studies on the influence of H₂S and SO₂ on the activity of a PdO/Al₂O₃ catalyst for removal of oxygen by total oxidation of (bio-)methane at very low O₂:CH₄ ratios, *Appl. Catal. B Environ.* 182 (2016) 550–561, <http://dx.doi.org/10.1016/j.apcatb.2015.09.026>.
- [23] R. Gholami, M. Alyani, K.J. Smith, Deactivation of Pd Catalysts by water during low temperature methane oxidation relevant to natural gas vehicle converters, *Catalysts* 5 (2015) 561–594, <http://dx.doi.org/10.3390/catal5020561>.
- [24] G.L. Rickett, V. Dupont, M.V. Twigg, Methane oxidation over palladium-wash-coated foils in the presence of sulphur dioxide, *Catal. Today* 155 (2010) 51–58, <http://dx.doi.org/10.1016/j.cattod.2009.03.013>.
- [25] R. Burch, F.J. Urbano, P.K. Loader, Methane combustion over palladium catalysts: the effect of carbon dioxide and water on activity, *Appl. Catal. Gen.* 123 (1995) 173–184, [http://dx.doi.org/10.1016/0926-860X\(94\)00251-7](http://dx.doi.org/10.1016/0926-860X(94)00251-7).
- [26] D.L. Mowery, M.S. Graboski, T.R. Ohno, R.L. McCormick, Deactivation of PdO-Al₂O₃ oxidation catalyst in lean-burn natural gas engine exhaust: aged catalyst characterization and studies of poisoning by H₂O and SO₂, *Appl. Catal. B Environ.* 21 (1999) 157–169, [http://dx.doi.org/10.1016/S0926-3373\(99\)00117-X](http://dx.doi.org/10.1016/S0926-3373(99)00117-X).
- [27] T.V. Choudhary, S. Banerjee, V.R. Choudhary, Catalysts for combustion of methane and lower alkanes, *Appl. Catal. Gen.* 234 (2002) 1–23, [http://dx.doi.org/10.1016/S0926-860X\(02\)00231-4](http://dx.doi.org/10.1016/S0926-860X(02)00231-4).
- [28] G. Lapisardi, L. Urfels, P. Gélin, M. Primet, A. Kaddouri, E. Garbowski, S. Toppi, E. Tena, Superior catalytic behaviour of Pt-doped Pd catalysts in the complete oxidation of methane at low temperature, *Catal. Today* 117 (2006) 564–568, <http://dx.doi.org/10.1016/j.cattod.2006.06.004>.
- [29] G. Lapisardi, P. Gélin, A. Kaddouri, E. Garbowski, S. Da Costa, Pt-Pd bimetallic catalysts for methane emissions abatement, *Top. Catal.* 42–43 (2007) 461–464, <http://dx.doi.org/10.1007/s11244-007-0225-8>.
- [30] K. Persson, L.D. Pfefferle, W. Schwartz, A. Ersson, S.G. Järås, Stability of palladium-based catalysts during catalytic combustion of methane: the influence of water, *Appl. Catal. B Environ.* 74 (2007) 242–250, <http://dx.doi.org/10.1016/j.apcatb.2007.02.015>.
- [31] H. Yamamoto, H. Uchida, Oxidation of methane over Pt and Pd supported on alumina in lean-burn natural-gas engine exhaust, *Catal. Today* 45 (1998) 147–151, [http://dx.doi.org/10.1016/S0920-5861\(98\)00265-X](http://dx.doi.org/10.1016/S0920-5861(98)00265-X).
- [32] N.M. Kinnunen, J.T. Hirvi, M. Suvanto, T.A. Pakkanen, Methane combustion activity of Pd-PdO_x-Pt/Al₂O₃ catalyst: the role of platinum promoter, *J. Mol. Catal. Chem.* 356 (2012) 20–28, <http://dx.doi.org/10.1016/j.molcata.2011.12.023>.
- [33] N.M. Kinnunen, J.T. Hirvi, K. Kallinen, T. Maunula, M. Keenan, M. Suvanto, Case study of a modern lean-burn methane combustion catalyst for automotive applications: what are the deactivation and regeneration mechanisms? *Appl. Catal. B Environ.* 207 (2017) 114–119, <http://dx.doi.org/10.1016/j.apcatb.2017.02.018>.
- [34] M. Honkanen, M. Kärkkäinen, T. Kolli, O. Heikkilä, V. Viitanen, L. Zeng, H. Jiang, K. Kallinen, M. Huuhtanen, R.L. Keiski, J. Lahtinen, E. Olsson, M. Vippola, Accelerated deactivation studies of the natural-gas oxidation catalyst—Verifying the role of sulfur and elevated temperature in catalyst aging, *Appl. Catal. B Environ.* 182 (2016) 439–448, <http://dx.doi.org/10.1016/j.apcatb.2015.09.054>.
- [35] K. Persson, A. Ersson, K. Jansson, J.L.G. Fierro, S.G. Järås, Influence of molar ratio on Pd-Pt catalyst for methane combustion, *J. Catal.* 243 (2006) 14–24, <http://dx.doi.org/10.1016/j.jcat.2006.06.019>.
- [36] H. Nassiri, K.-E. Lee, Y. Hu, R.E. Hayes, R.W.J. Scott, N. Semagina, Platinum inhibits low-temperature dry lean methane combustion through palladium reduction in Pd- $\text{Pt}/\text{Al}_2\text{O}_3$: an *in situ* X-ray absorption study, *Chem. Phys. Chem.* 18 (2017) 238–244, <http://dx.doi.org/10.1002/cphc.201600993>.
- [37] P. Castellazzi, G. Groppi, P. Forzatti, Effect of Pt/Pd ratio on catalytic activity and redox behavior of bimetallic Pt-Pd/Al₂O₃ catalysts for CH₄ combustion, *Appl. Catal. B Environ.* 95 (2010) 303–311, <http://dx.doi.org/10.1016/j.apcatb.2010.01.008>.
- [38] N. Sadokhina, G. Smedler, U. Nyblén, M. Olofsson, L. Olsson, The influence of gas composition on Pd-based catalyst activity in methane oxidation - inhibition and promotion by NO, *Appl. Catal. B Environ.* 200 (2017) 351–360, <http://dx.doi.org/10.1016/j.apcatb.2016.07.012>.
- [39] N. Sadokhina, F. Ghasempour, X. Auveray, G. Smedler, U. Nyblén, M. Olofsson, L. Olsson, An experimental and kinetic modelling study for methane oxidation over Pd-based catalyst: inhibition by water, *Catal. Lett.* 147 (2017) 2360–2371, <http://dx.doi.org/10.1007/s10562-017-2133-2>.
- [40] A.T. Gremminger, H.W. Pereira de Carvalho, R. Popescu, J.-D. Grunwaldt, O. Deutschmann, Influence of gas composition on activity and durability of bimetallic Pd-Pt/Al₂O₃ catalysts for total oxidation of methane, *Catal. Today* 258 (2015) 470–480, <http://dx.doi.org/10.1016/j.cattod.2015.01.034>.
- [41] Y. Ozawa, Y. Tochihara, A. Watanabe, M. Nagai, S. Omi, Deactivation of Pt-PdO/Al₂O₃ in catalytic combustion of methane, *Appl. Catal. Gen.* 259 (2004) 1–7, <http://dx.doi.org/10.1016/j.apcata.2003.09.029>.
- [42] D. Ciuparu, E. Perkins, L. Pfefferle, In situ DR-FTIR investigation of surface hydroxyls on γ -Al₂O₃ supported PdO catalysts during methane combustion, *Appl. Catal. Gen.* 263 (2004) 145–153, <http://dx.doi.org/10.1016/j.apcata.2003.12.006>.
- [43] D. Ciuparu, N. Katsikis, L. Pfefferle, Temperature and time dependence of the water inhibition effect on supported palladium catalyst for methane combustion, *Appl. Catal. Gen.* 216 (2001) 209–215, [http://dx.doi.org/10.1016/S0926-860X\(01\)00558-0](http://dx.doi.org/10.1016/S0926-860X(01)00558-0).
- [44] P. Hurtado, S. Ordóñez, H. Saastre, F.V. Díez, Development of a kinetic model for the oxidation of methane over Pd/Al₂O₃ at dry and wet conditions, *Appl. Catal. B Environ.* 51 (2004) 229–238, <http://dx.doi.org/10.1016/j.apcatb.2004.03.006>.
- [45] C.F. Cullis, B.M. Willatt, Oxidation of methane over supported precious metal catalysts, *J. Catal.* 83 (1983) 267–285, [http://dx.doi.org/10.1016/0021-9517\(83\)90054-4](http://dx.doi.org/10.1016/0021-9517(83)90054-4).
- [46] R. Burch, P.K. Loader, Investigation of Pt/Al₂O₃ and Pd/Al₂O₃ catalysts for the combustion of methane at low concentrations, *Appl. Catal. B Environ.* 5 (1994) 149–164, [http://dx.doi.org/10.1016/0926-3373\(94\)00037-9](http://dx.doi.org/10.1016/0926-3373(94)00037-9).
- [47] S.H. Oh, P.J. Mitchell, R.M. Siewert, Methane oxidation over alumina-supported noble metal catalysts with and without cerium additives, *J. Catal.* 132 (1991) 287–301, [http://dx.doi.org/10.1016/0021-9517\(91\)90149-X](http://dx.doi.org/10.1016/0021-9517(91)90149-X).
- [48] C. Carrillo, T.R. Johns, H. Xiong, A. DeLaRiva, S.R. Challa, R.S. Goeka, K. Artyushkova, W. Li, C.H. Kim, A.K. Datye, Trapping of Mobile Pt species by PdO nanoparticles under oxidizing conditions, *J. Phys. Chem. Lett.* 5 (2014) 2089–2093, <http://dx.doi.org/10.1021/jz5009483>.
- [49] X. Weng, H. Ren, M. Chen, H. Wan, Effect of surface oxygen on the activation of methane on palladium and platinum surfaces, *ACS Catal.* 4 (2014) 2598–2604, <http://dx.doi.org/10.1021/cs500510x>.
- [50] H. Nassiri, K.-E. Lee, Y. Hu, R.E. Hayes, R.W.J. Scott, N. Semagina, Water shifts PdO-catalyzed lean methane combustion to Pt-catalyzed rich combustion in Pd-Pt catalysts: *in situ* X-ray absorption spectroscopy, *J. Catal.* 352 (2017) 649–656, <http://dx.doi.org/10.1016/j.jcat.2017.06.008>.
- [51] F. Arosio, S. Colussi, G. Groppi, A. Trovarelli, Regeneration of S-poisoned Pd/Al₂O₃ catalysts for the combustion of methane, *Catal. Today* 117 (2006) 569–576, <http://dx.doi.org/10.1016/j.cattod.2006.06.006>.
- [52] F. Arosio, S. Colussi, A. Trovarelli, G. Groppi, Effect of alternate CH₄-reducing/lean combustion treatments on the reactivity of fresh and S-poisoned Pd/CeO₂/Al₂O₃ catalysts, *Appl. Catal. B Environ.* 80 (2008) 335–342, <http://dx.doi.org/10.1016/j.apcatb.2007.11.030>.
- [53] A. Gremminger, P. Lott, M. Merts, M. Casapu, J.-D. Grunwaldt, O. Deutschmann, Sulfur poisoning and regeneration of bimetallic Pd-Pt methane oxidation catalysts, *Appl. Catal. B Environ.* 218 (2017) 833–843, <http://dx.doi.org/10.1016/j.apcatb.2017.06.048>.
- [54] N. Oktar, J. Mitome, E.M. Holmgreen, U.S. Ozkan, Catalytic reduction of N₂O and NO_x with methane over sol-gel palladium-based catalysts, *J. Mol. Catal. Chem.* 259 (2006) 171–182, <http://dx.doi.org/10.1016/j.molcata.2006.06.024>.
- [55] J.F. Moulder, W.F. Stickle, P.E. Sobol, K.D. Bomben, *Handbook of X-ray Photoelectron Spectroscopy*, Perkin-Elmer Corporation, Eden Prairie, 1992.
- [56] Y. Ji, T.J. Toops, U.M. Graham, G. Jacobs, M. Crocker, A kinetic and DRIFTS study of supported Pt catalysts for NO oxidation, *Catal. Lett.* 110 (2006) 29–37, <http://dx.doi.org/10.1007/s10562-006-0100-4>.
- [57] T. Hamzehlooyan, C.S. Sampara, J. Li, A. Kumar, W.S. Epling, Kinetic study of adsorption and desorption of SO₂ over γ -Al₂O₃ and Pt/ γ -Al₂O₃, *Appl. Catal. B Environ.* 181 (2016) 587–598, <http://dx.doi.org/10.1016/j.apcatb.2015.08.003>.
- [58] O. Saur, M. Benisiel, A.B.M. Saad, J.C. Lavalle, C.P. Tripp, B.A. Morrow, The structure and stability of sulfated alumina and titania, *J. Catal.* 99 (1986) 104–110, [http://dx.doi.org/10.1016/0021-9517\(86\)90203-4](http://dx.doi.org/10.1016/0021-9517(86)90203-4).
- [59] M.B. Mitchell, V.N. Sheinker, M.G. White, Adsorption and reaction of sulfur dioxide on alumina and sodium-impregnated alumina, *J. Phys. Chem.* 100 (1996) 7550–7557, <http://dx.doi.org/10.1021/jp9519225>.
- [60] M.S. Wilburn, W.S. Epling, SO₂ adsorption and desorption characteristics of Pd and Pt catalysts: precious metal crystallite size dependence, *Appl. Catal. Gen.* 534 (2017) 85–93, <http://dx.doi.org/10.1016/j.apcata.2017.01.015>.